Supplemental Document

Optics Letters

Spectrally resolved wedged reversal shearing interferometer: supplement

BILLY LAM AND CHUNLEI GUO*

The Institute of Optics, University of Rochester, Rochester, New York 14627, USA
**Corresponding author: guo@optics.rochester.edu*

Supplement DOI: https://doi.org/10.6084/m9.figshare.14229905

Parent Article DOI: https://doi.org/10.1364/OL.417997

Spectrally-resolved wedged reversal shearing interferometer: Supplementary Materials

BILLY LAM, AND CHUNLEI GUO*

The Institute of Optics, University of Rochester, Rochester, New York, 14627, USA
** Corresponding author: guo@optics.rochester.edu*

Abstract: This document provides supplementary information to "Spectrally-resolved wedged reversal shearing interferometer." This document explains the generalized phase-shifting interferometry (GPSI) that is required for the phase retrieval of the spectrally-resolved WRSI shearing interferograms. Then the full derivation for the wavefront extraction of the spectrally-resolved WRSI shearing interferograms is provided.

1. Generalized PSI

The spectrally-resolved WRSI interferogram as a function of the mirror position can be written as

$$\tilde{I}(x_m, x, y, \nu) = \tilde{I}(x, y, \nu)[1+\cos(2\pi \nu x_m)]\,. \tag{S1}$$

The intensity that is measured at the detector is

$$I(x_m, x, y) = \int_0^\infty \tilde{I}(x_m, x, y, \nu) d\nu = \int_0^\infty \tilde{I}(x, y, \nu)[1+\cos(2\pi \nu x_m)] d\nu\,. \tag{S2}$$

This is just a Fourier cosine transform. The inverse gives us the desired spectrally-resolved WRSI interferogram

$$\tilde{I}(x, y, \nu) = 4\int_0^\infty \left[I(x_m, x, y) - \frac{1}{2} I(0, x, y) \right] \cos(2\pi \nu x_m) dx_m\,. \tag{S3}$$

For a certain frequency ν of the WRSI shearing interferograms, the k different phase shifts can be represented as

$$\tilde{I}_k(x, y, \nu) = \tilde{I}_0(x, y, \nu)\{1+\alpha(x, y, \nu)\cos[\phi_{WRSI}(x, y, \nu)+\psi_k]\}\,. \tag{S4}$$

For a fixed point on the measurement plane, we rewrite the intensity as

$$\begin{aligned} \tilde{I}_k &= \tilde{I}_0 + \tilde{I}_0 \alpha \cos\phi_{WRSI} \cos\psi_k - \tilde{I}_0 \alpha \sin\phi_{WRSI} \sin\psi_k \\ &= a_0 + a_1 \cos\psi_k + a_2 \sin\psi_k \end{aligned}\,. \tag{S5}$$

For a total of N phase-shifts, the least square (figure of merit) is

$$E = \sum_{k=0}^{N-1} (\tilde{I}_k - \hat{I}_k)^2 = \sum_{k=0}^{N-1} (a_0 + a_1 \cos\psi_k + a_2 \sin\psi_k - \hat{I}_k)^2 \tag{S6}$$

where $\widehat{I_k}$ is the measured intensity. To find the coefficients a_0, a_1, a_2 and minimize criterion E, we write in matric form

$$\mathbf{A}(\psi_0,...,\psi_N)\mathbf{a} \ = \mathbf{b}(\psi_0,...,\psi_N) \tag{S7}$$

where

$$\mathbf{A}(\psi_0,...,\psi_N) \ = \begin{pmatrix} N & \sum_{k=0}^{N-1}\cos\psi_k & \sum_{k=0}^{N-1}\sin\psi_k \\ \sum_{k=0}^{N-1}\cos\psi_k & \sum_{k=0}^{N-1}\cos^2\psi_k & \sum_{k=0}^{N-1}\cos\psi_k \sin\psi_k \\ \sum_{k=0}^{N-1}\sin\psi_k & \sum_{k=0}^{N-1}\cos\psi_k \sin\psi_k & \sum_{k=0}^{N-1}\sin^2\psi_k \end{pmatrix}, \tag{S8}$$

$$\mathbf{a} \ = \begin{pmatrix} a_0 \\ a_1 \\ a_2 \end{pmatrix} \tag{S9}$$

and

$$\mathbf{b}(\psi_0,...,\psi_N) \ = \begin{pmatrix} \sum_{k=0}^{N-1}\hat{I}_k \\ \sum_{k=0}^{N-1}\hat{I}_k \cos\psi_k \\ \sum_{k=0}^{N-1}\hat{I}_k \sin\psi_k \end{pmatrix}. \tag{S10}$$

Solving for the coefficients, we obtain

$$\mathbf{a} = \mathbf{A}^{-1}\mathbf{b}. \tag{S11}$$

The phase is then $\phi_{WRSI} = -\tan^{-1}\left(\frac{a_2}{a_1}\right)$.

Repeat this calculation for all (x, y) and we get $\phi_{WRSI}(x, y)$.

2. Phase-shifts selection for Generalized PSI

For phase shifting interferometry for a single wavelength, it is very simple to select the phase shifts. Most of the time multiple steps of equal phase-shifts are used. As minimal of 3 phase-shifts are needed because there are 3 unknowns in the two-beam interference equation. This selection works very well for single wavelength because the phase calculation can be made very simple, such as the 4-bin phase-shifting.

However, this is not the case for a spectrally-resolved phase shifting interferometry. When the phase-shift is induced by adjusting an arm length in an interferometer, the phase-shift induced scales inversely with the wavelength. This can cause repeats of phase-shifts modulo 2π for shorter wavelengths. For example, The $0, \pi/2, \pi, 3\pi/2$ (fourth roots of unity) 4-bin phase-shifting for the wavelength of 800nm would have two pairs of identical phase-shifts (0, π, 0, π) for the wavelength of 400nm (second harmonic), which is detrimental and fails to provide enough information to extract the phase. The four phase shifts of $0, \pi/2, \pi, 3\pi/2$ for the wavelength of 800nm starts to have identical phase shifts for wavelengths less than 600 nm. Because the bandwidth of our simulated pulses does not include 600 nm, we choose the phase shift of $0, \pi/2, \pi, 3\pi/2$ for the central wavelength 800 nm. If the bandwidth is large with certain wavelengths having repeated phase shifts, the phase shifts must be re-selected.

3. Wavefront extraction of spectrally-resolved WRSI shearing interferograms.

After the phase retrieval, it's important to extract the wavefront. This can be done by manipulating the phase. Recalls that the phase of the WRSI at a certain natural frequency ω with the shearing direction of $\hat{x}$ is

$$\phi^x(x,y;s) = c_0 + c_1 y + s\frac{\partial W_{ox}}{\partial x} - s\frac{\partial W_{ex}}{\partial x} + 2W_{ox}(x,y). \tag{S12}$$

where s is the shearing amount in the $+\hat{x}$ direction, the subscript ox denotes odd order of x and ex denotes even order of x. The first two terms are due to the geometry of the setup where one of the entrance faces of the beam splitter cube (BSC) has a y-wedge angle. By measuring the phase of an interferogram with $s = 0$, we will obtain

$$\phi^x(x,y;s=0) = c_0 + c_1 y + 2W_{ox}(x,y). \tag{S13}$$

By Eq. (S13) and the property of odd function ($W_{ox}(0,y) = 0$), we can solve for the odd component of the wavefront. The solution is

$$W_{ox}(x,y) = \frac{\phi^x(x,y;s=0) - \phi^x(0,y;s=0)}{2}. \tag{S14}$$

Now we isolate the derivative of the wavefront by subtracting Eq. (S12) by (S13):

$$\phi^x(x,y;s=s_x) - \phi^x(x,y;s=0) = s_x\frac{\partial W_{ox}}{\partial x} - s_x\frac{\partial W_{ex}}{\partial x}. \tag{S15}$$

Numerically integrating the above equation and dividing by s_x yields

$$W_{ox}(x,y) - W_{ex}(x,y) = \int_0^x \left(\frac{\phi^x(x',y;s=s_x) - \phi^x(x',y;s=0)}{s_x} \right) dx'. \tag{S16}$$

The even component of the wavefront can be computed by subtracting Eq. (S14) by Eq. (S16):

$$\begin{aligned} W_{ex}(x,y) &= \frac{\phi^x(x,y;s=0) - \phi^x(0,y;s=0)}{2} \\ &- \int_0^x \left(\frac{\phi^x(x',y;s=s_x) - \phi^x(x',y;s=0)}{s_x} \right) dx' \end{aligned} \tag{S17}$$

The total wavefront is

$$W(x,y) = W_{ox}(x,y) + W_{ex}(x,y) + f(y). \tag{S18}$$

where $f(y) = W_{oy}(0,y) + W_{ey}(0,y)$. These wavefront components can be calculated using the interferogram with the shearing direction of $\hat{y}$ following the same derivation above. Their expressions are

$$W_{oy}(0,y)=\frac{\phi^{y}(0,y;s=0)-\phi^{y}(0,0;s=0)}{2}, \tag{S19}$$

and

$$\begin{aligned}W_{ey}(0,y)&=\frac{\phi^{y}(0,y;s=0)-\phi^{y}(0,0;s=0)}{2}\\&-\int_{0}^{y}\left(\frac{\phi^{y}(0,y';s=s_y)-\phi^{y}(0,y';s=0)}{s_y}\right)dy'\end{aligned}. \tag{S20}$$

where s_y is the shearing amount in the $\hat{y}$ direction and should be equal to s_x. Adding up all of the odd and even components in Eq. (14, 17, 19, 20) will give us the total wavefront by Eq. (18). However, because the interferograms of our WRSI only consists of half of the beam, we only obtain the total wavefront in the first quadrant. To obtain the wavefront in all four quadrants, we utilize the property of odd and even function to get

$$W(\pm x,y)=\pm W_{ox}(x,y)+W_{ex}(x,y)+W_{oy}(0,y)+W_{ey}(0,y), \tag{S21}$$

and

$$W(\pm x,-y)=\pm W_{ox}(x,y)+W_{ex}(x,y)-W_{oy}(0,y)+W_{ey}(0,y). \tag{S22}$$

where $x > 0$ and $y > 0$. As a summary, the wavefront in the four quadrants are extracted using the four phase distributions $\phi^{x}(x,y;s=0), \phi^{x}(x,y;s=s_x), \phi^{y}(x,y;s=0)$, and $\phi^{y}(x,y;s=s_y)$. The phase retrieval and wavefront extraction are done using our Matlab code that is available upon request. The Matlab code for phase unwrapping is taken from Ref. 42 and 43.

4. Data acquisition and post-processing time

To extract all electric field $E(x,y,\omega)$ information, a total of 9 autocorrelation measurements are required. In our experiment, each scan consists of 1500 frames at 30 frames per second as shown in Visualization 7. Therefore, the data acquisition time, which is proportional to the coherence length of the pulse, is about 450 seconds. To increase the data acquisition speed, we can increase the 23.5 nm step size of the scan (47 nm optical path difference) up to the Nyquist limit of about 180 nm step size and reduce the total number of frames as many are beyond the coherence length. The post-processing time is comparable excluding the step of converting the 3-dimensional result of $E(x,y,\omega)$ to a 4-dimensional representation of $E(x,y,z,t)$. Note that $E(x,y,\omega)$ already contain the full information of the pulse.

5. Other input polarization states

The technique described can also be applied to arbitrary input polarization states. This can be achieved by measuring the amplitude and phase of the electric field for the horizontal and vertical polarization state individually ($E_H(x,y,\omega), E_V(x,y,\omega), \phi_H(x,y,\omega)$, and $\phi_V(x,y,\omega)$), along with an additional retardance measurement at a single wavelength (

$\phi_H(x, y, \omega_0) - \phi_V(x, y, \omega_0)$). This additional measurement allows the retardance to be deduced at all wavelengths.

6. Spectral phase measurement

The spectral phase of the pulse in Fig. 3 of the main manuscript is measured using FROG from Swamp Optics. The result is shown in Fig. S1, showing a parabolically-shaped spectral phase.

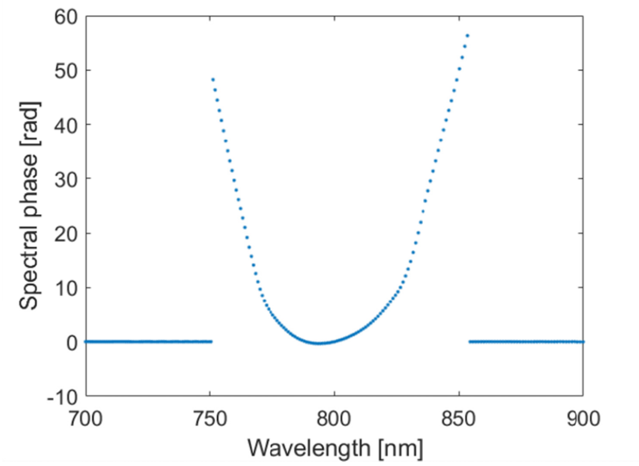

Fig. S1 Spectral phase of the pulse in Fig. 3 of the main manuscript by a FROG measurement.

References

42. M. A. Herráez, D. R. Burton, M. J. Lalor, and M. A. Gdeisat, "Fast two-dimensional phase-unwrapping algorithm based on sorting by reliability following a noncontinuous path," Applied optics **41**, 7437-7444 (2002).2.2.

43. M. F. Kasim, "Fast 2D phase unwrapping implementation in matlab," 2017, https://github.com/mfkasim91/unwrap_phase/.